Real-Time Analysis of GaSb(001) during Sb Desorption by Core-Level Photoelectron Spectroscopy

Fumihiko Maeda,* Yoshio Watanabe,* and Masaharu Oshima†

NTT Interdisciplinary Research Laboratories, 3-9-11 Midoricho, Musashino-shi, Tokyo 180, Japan

(Received 8 April 1996)

GaSb(001) surfaces during an Sb desorption process at substrate-temperature-dependent growth conditions were analyzed by measuring core-level photoelectron spectra in real time, which can provide surface bonding information that supplements structural information. The time dependence of the Ga 3*d* intensity revealed that Sb desorption from GaSb(001) can be explained by two competing processes with fast and slow time constants. By analyzing the Sb 4*d* and Ga 3*d* spectra at various stages during Sb desorption at the growth temperature, we find that Sb atoms occupy different sites in the top layer of Sb double layers, which correlates well with fast and slow time constants. [S0031-9007(97)03231-6]

PACS numbers: 68.45.Da, 82.65.My, 87.64.Lg

Core-level photoelectron spectroscopy (PES) with synchrotron radiation (SR) is a powerful method to analyze surface bonding states. Therefore many researchers have attempted to analyze the surface change in real time by this method. However, this method has not been applied to observations in growing surface changes occurring during periods of several seconds during molecular beam epitaxy because a time resolution of less than a second for a spectrum is needed, although that is, so far, at least several seconds [1]. Therefore we have developed a novel real-time analysis system that uses core-level PES excited by vacuum-ultraviolet light (VUV) and measured by a "nonscanning measuring method." In this Letter, we report the substrate temperature dependence of Sb desorption and clarify the Sb bonding state on the GaSb surface at growth substrate temperature by using the first real-time core-level PES investigation with subsecond time resolution on GaSb(001) to demonstrate the effectiveness of this investigation.

Experiments were performed using a real-time crystal growth analysis system that uses synchrotron radiation photoelectron spectroscopy. A growth-analysis apparatus was developed for this system [2], in which photoelectron spectra can be measured every 100 ms by an angle-integrated type hemispherical photoelectron analyzer with an electrostatic lens. The acquisition time of the conventional photoelectron measuring system is at most several seconds [1]. Our short acquisition time was achieved by nonscanning measuring methods that allow the acquisition of snapshot photoelectron spectra without the need for kinetic energy scanning by an electrostatic lens. Although the photoelectron analyzer is a conventional one, a new 114-channel multichannel detection system with a resistive anode is needed for this system. Furthermore, VUV light from the beam line of ABL-3B [3] at the normal-conducting accelerating ring (NAR) [4] of NTT SOR is used for this system. Details are described in Ref. [2].

The samples were *n*-type GaSb(001). A buffer layer about 200 Å thick was grown at 500 °C with a III/V flux ration of 1:10. A streaky, clear $c(2 \times 6)$ reflection high-energy electron diffraction pattern was obtained at room temperature and real-time analysis experiments were carried out using this surface.

For the real-time analysis of Sb desorption, the experimental sequence is as follows: The substrate was heated from 380 °C to 610 °C under Sb flux of 2.5×10^{-7} Torr, which was measured at the sample growth/measurement position. After the substrate temperature became stable, Ga 3*d* or Sb 4*d* PES measurements were started. On this occasion, Sb flux was supplied. When 20 s had passed from the beginning of PES measurement, the Sb flux was stopped. Then PES measurements were continued for 130 s. Under the same conditions during the same sequence, only 1×3 was observed at the substrate temperature over 500 °C and 1×3 and $c(2 \times 6)$ were observed below 500 °C. At 380 °C, 2×5 was observed in addition to 1×3 and $c(2 \times 6)$. The photon energy was calibrated by Au Fermi level measurement, and the total energy resolution was determined to be 0.3 to 0.4 eV. The typical photon flux was 7×10^9 photons/s estimated by the photocurrent with a Au mesh. Because the counting rate decreases over 5×10^4 count per second (cps) due to a large dead time, we set the appropriate size slit of the electron analyzer to a counting rate of $2-3 \times 10^4$ cps. These high counting rates are due to the large cross sections of Sb 4*d* and Ga 3*d* for the photon energy of 90 eV. Typical data accumulation time is 0.5 s to obtain a full spectrum for Fig. 1 and three spectra were used for a spectrum in Fig. 2.

Figure 1(a) shows the time dependence of Ga 3*d* photoelectron intensities at a substrate temperature of 520 °C. These Ga 3*d* photoelectron intensities are defined and calculated by the sum of the electron intensity data of photoelectron spectra corresponding to binding energies. Although the Ga 3*d* intensity was constant during Sb supply, the intensity increased and saturated after the Sb supply was stopped. The saturation of the Ga 3*d* intensity indicates that Sb atoms, which are adsorbed on the surface during Sb supply, are completely desorbed. When Sb was supplied again, the intensity immediately recovered to

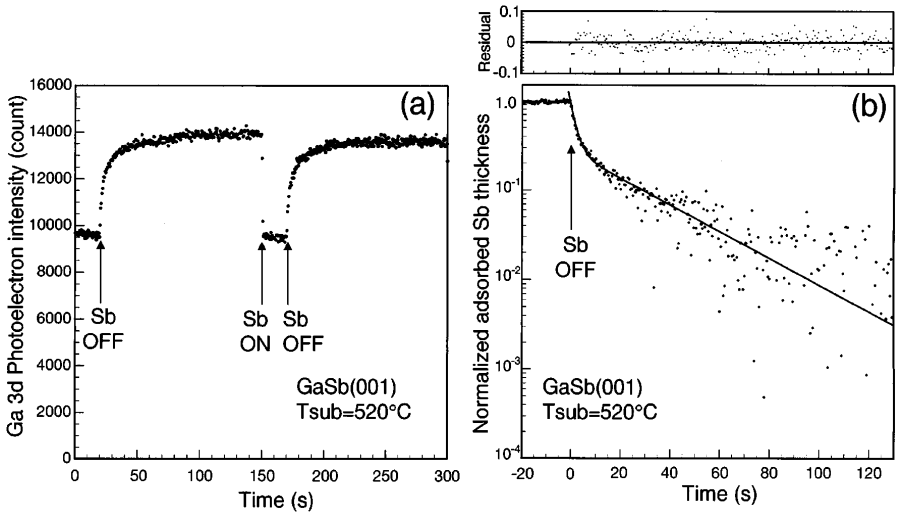

FIG. 1. Time dependence of (a) Ga 3*d* photoelectron intensity and (b) normalized Sb thickness transformed by Eq. (2) described in the text. The solid curve in the right-hand-side figure is the fitting result for Eq. (3) with time constants $\tau_1 = 2.37$ s and $\tau_2 = 29.1$ s. The residual between the transformed data and the fitted curve is shown at the top of (b).

the same intensity as that during the previous Sb supply. These changes occurred repetitively when the sequence was continued. From the viewpoint of taking a completely Sb-desorbed surface as a base, the adsorbed Sb atoms can be called excess Sb atoms. This intensity change can be expressed by the desorption of these excess Sb atoms. To analyze the desorption process, the normalized thickness of these excess Sb atoms is introduced. Because of photoelectron attenuation, the Ga 3*d* photoelectron intensity data $I(t)$ are expressed as a function of excess Sb-adsorbed thickness on the completely Sb-desorbed GaSb surface $d(t)$ as follows:

$$I(t) = I_\infty \exp\left(-\frac{d(t)}{\lambda}\right), \tag{1}$$

where t is the time passed from the point "Sb off," λ is the mean-free path of Ga 3*d* photoelectrons, and I_∞ is equal to $I(\infty)$. When d_0 is defined as the Sb thickness difference on the GaSb topmost surface between the point "Sb flux on" and that of "Sb flux off," $d(0) = d_0$ and $d(\infty) = 0$. Hence normalized Sb thickness is given by

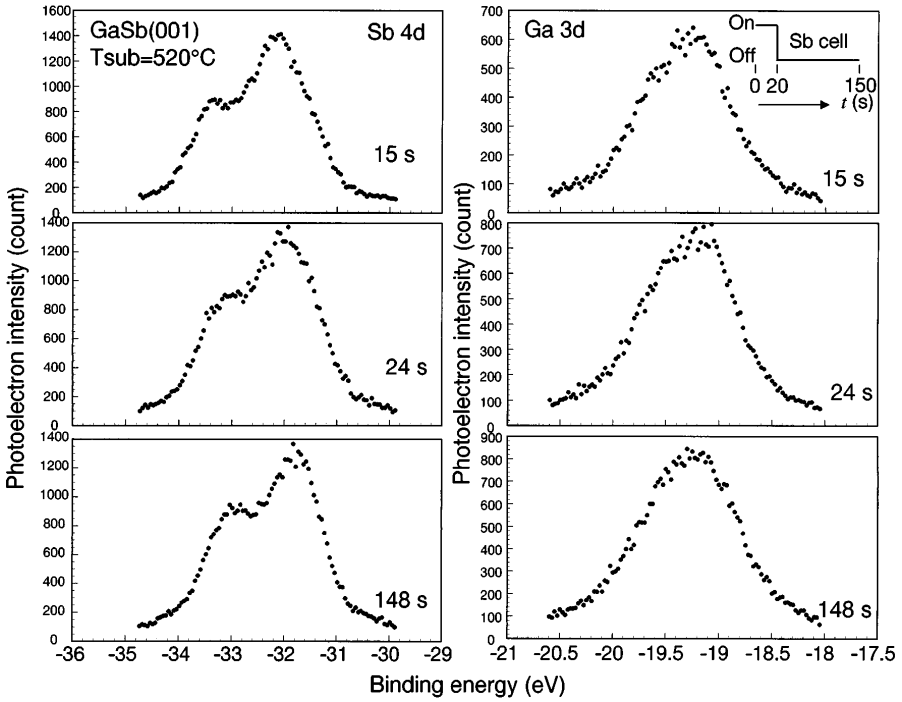

FIG. 2. Sb 4*d* and Ga 3*d* photoelectron spectra under Sb flux and during Sb desorption. Each spectrum consists of the sum of three spectra recorded over consecutive intervals of 0.5 s, starting 0.5 s before the time indicated to the right of each spectrum.

$$\frac{d(t)}{d_0} = \ln\left(\frac{I(t)}{I_\infty}\right)\Big/\ln\left(\frac{I_0}{I_\infty}\right), \quad (2)$$

where I_0 is equal to $I(0)$. Figure 1(b) shows the normalized thickness of the excess Sb as a function of time, which is transformed from Fig. 1(a) using Eq. (2). Here the intensities of I_0 and I_∞, respectively, are used for the values averaged from 0 to 19 s and 130 to 145 s. The horizontal axis is shifted by -20 s to make the time of Sb flux off equal to zero.

If the normalized Sb thickness decreases exponentially with a single time constant, it should be possible to fit a straight line to the data in Fig. 1(b). However, it is clear that the data in this figure does not lie on a single straight line, indicating that this normalized Sb thickness changes with more than two time constants. Two straight lines, in particular, can be recognized on 0–4 and 32–150 s in Fig. 1(b). To obtain the gradient of these two lines, we have assumed two time constants and fitted the experimental data by using the following equation:

$$\frac{d(t)}{d_0} = \frac{d(t)}{d_1 + d_2} = \frac{d_1}{d_1 + d_2}\exp\left(-\frac{t}{\tau_1}\right) + \frac{d_2}{d_1 + d_2}\exp\left(-\frac{t}{\tau_2}\right), \quad (3)$$

where d_1 and d_2 are Sb layer thicknesses whose time constants for desorption are τ_1 and τ_2, respectively. By fitting Eq. (3) to Fig. 1(b), τ_1 and τ_2 are determined to be 2.37 and 29.1 s, respectively. This shows that on GaSb(001), at the growth temperature with Sb flux exposure, Sb atoms occupy two Sb sites, which can be related to the fast and slow desorptions.

These procedures were also performed on other data with substrate temperatures from 380 °C to 610 °C, and the time constants obtained are summarized in Fig. 3. By fitting these data, activation energy is estimated to be 0.78 eV for fast desorption and 0.87 eV for slow desorption. Here the sum of the calculated thicknesses, d_1 and d_2, for the various substrate temperatures is at most 0.5 ML. Hence Eq. (1) is a good approximation but is not precisely accurate. Therefore, to verify the validity of these activation energies, we analyzed the time-dependence data of Ga $3d$ photoelectron intensities at various substrate temperatures, such as those in Fig. 1(a), again by using the following equation, which is also a good approximation to estimate surface adsorbate coverage $\theta(t)$:

$$I(t) = I_{\mathrm{Sb}}\theta(t) + I_{\mathrm{Ga}}(1 - \theta(t)) = I_{\mathrm{Sb}}\left\{\theta_1\exp\left(-\frac{t}{\tau_1}\right) + \theta_2\exp\left(-\frac{t}{\tau_2}\right)\right\} + I_{\mathrm{Ga}}\left\{1 - \theta_1\exp\left(-\frac{t}{\tau_1}\right) - \theta_2\exp\left(-\frac{t}{\tau_2}\right)\right\}, \quad (4)$$

where I_{Ga} is the Ga $3d$ intensity for the Ga-full surface [2], I_{Sb} is that for the surface fully covered with Sb, and θ_1 and θ_2 are Sb layer coverages whose time constants for desorption are τ_1 and τ_2, respectively. By fitting the time-dependence data of photoelectron intensities at various substrate temperatures, such as those in Fig. 1(a), using Eq. (4), activation energies of 0.69 and 0.90 eV are obtained. Therefore these estimated values more than the first decimal place of the activation energies are reliable independent of calculation models. Thus these values are much larger than the activation energy of physisorption, indicating that physisorbed Sb_4 molecules were not detected and the number of Sb_4 molecules was negligibly small. Therefore the excess Sb atoms were found to be chemisorbed on the GaSb surface.

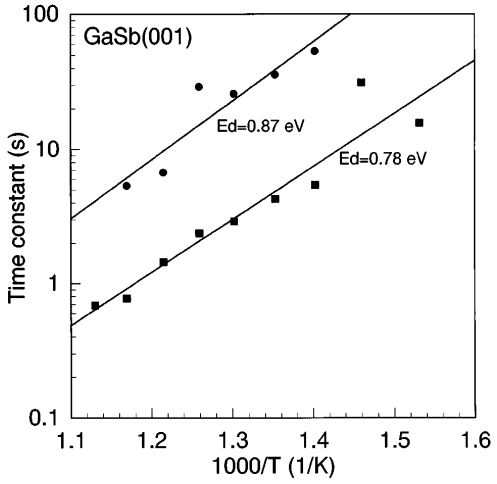

FIG. 3. Plot of time constant vs substrate temperature. ■ and ● are data for τ_1 and τ_2, respectively. The solid lines are fitted results for activation energy E_d.

To clarify the bonding state of these chemisorbed Sb atoms, we analyzed the changes in Ga $3d$ and Sb $4d$ photoelectron spectra. Figure 2 shows Sb $4d$ and Ga $3d$ photoelectron spectra at 15, 24, and 148 s after the PES measurement was started at a substrate temperature of 520 °C. Since the Sb supply was stopped at 20 s, the 15-s spectra are typical for the surface with Sb supply. The spectra at 24 s represent the surface 4 s after Sb supply was stopped, and this time of 24 s is selected for the transient state. Since 4 s is almost double the period of the time constant for the fast desorption τ_1, the Sb of the fast desorption site was almost completely desorbed. However, 4 s is far smaller than τ_2, and almost all the Sb slow desorption sites remain. Therefore 4 s is thought to be suitable for distinguishing the fast desorption from the slow desorption. The spectra at 148 s represent the surface of the saturated point of the Ga $3d$ intensity.

Figure 4 shows the difference spectra of Sb $4d$ and Ga $3d$ from Fig. 2. (A core-level shift of 0.1 eV was found when the substrate temperature changed from room temperature to around 500 °C, and no core-level shift was observed when compared with the Sb supply stage and the Sb completely desorbed stage.) Since these spectrum intensities are weak due to the difference between the two spectra, quantitative analysis is difficult. However, the intensity is sufficient for analyzing peak position using

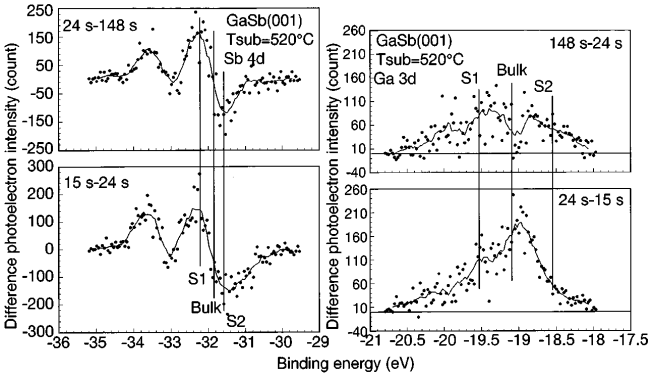

FIG. 4. Difference photoelectron spectra of Sb 4*d* and Ga 3*d* in Fig. 2. The solid lines are the smoothed result of the nearest nine points.

the smoothed results indicated by solid lines in the figure. In this figure, the bottom spectra show the differences between the stable state under Sb flux exposure and the transient state during Sb desorption, and the top spectra show the difference between the transient state and saturated state during Sb desorption. The binding energy position of the bulk and surface components of Sb $4d_{5/2}$ and Ga $3d_{5/2}$ are indicated on each difference spectrum as Bulk, S1, and S2 [5].

In the difference spectra of Sb 4*d*, a peak is located at the S1 position and a trough is located at the S2 position in both spectra. The S1 component of Sb $4d_{5/2}$ can be assigned to the topmost Sb atoms of two Sb layers [5]. Since these spectra are obtained by subtracting a later time spectrum from an earlier time spectrum, the peak shows that the species disappeared and the trough shows that they appeared. Therefore these difference spectra of Sb 4*d* indicate that the excess Sb atoms assigned to the topmost Sb site of Sb double layers decreased by Sb desorption although it is not known whether Sb atoms desorb from the adsorbed sites directly or from appropriate specific sites such as a step edge. This shows that Sb atoms occupy the topmost Sb site of Sb double layers formed due to excess Sb atom adsorption under growth conditions. Moreover, the intensity of the S2 component increases and that of the bulk component changes little with the topmost Sb desorption. These differences are consistent with the change on $d_{3/2}$ at around 33.5 eV.

On the other hand, in the difference spectra of Ga 3*d*, the features are different from each other. Since these spectra are obtained by subtracting an earlier time spectrum from a later time spectrum—which is opposite to the Sb 4*d* case—the peak shows that the species appeared and the trough shows that they disappeared. In the bottom spectra, a prominent peak, which is almost a single Ga 3*d* bulk component [5] composed of $3d_{3/2}$ and $3d_{5/2}$, can be distinguished and the difference intensities at S1 and S2 [5] are very weak. In the top spectrum, the difference intensity is very weak at the bulk position compared with the bottom spectrum and a non-negligible intensity is seen at the surface component positions S1 and S2. These results show that the surface components tend to be large in the top difference spectrum, while the difference spectra of Ga 3*d* are not only from bulk or surface components. Here the increase in intensity in the bulk component shows that no charge is transferred to the third layer (Ga) atoms underlying second layer (Sb) atoms. The increase in intensity in the surface component shows that the charge is transferred to the third layer (Ga) atoms. From the viewpoint of these charge transfers, the different shape of the difference spectra indicates that the surface bonding is not the same between the early and late desorption stages.

These results indicate that two types of Sb occupied sites exist which are related to the slow and fast desorptions. In this case, the two types of sites do not only mean two atomic positions of a unit cell, but means, in addition, any different sites that appear at a real surface such as kinks, step edges, and some positions whose bonding states are mentioned above. Thus we found that chemical bonding change induced by the two types of Sb desorption can be observed by our real-time analysis, although they are not induced by the change of surface superstructure. These fast and slow reactions were distinguished for the first time by the subsecond resolution of photoelectron spectroscopy. We showed the possibility of site-specific analysis by real-time bonding analysis using core-level photoelectron spectroscopy, which can provide supplementary information in addition to structural information.

We would like to thank Retsu Oiwa, Hideo Iwai, Masami Taguchi, and Yoshiteru Kita of ULVAC PHI Inc. for designing and assembling a new multichannel detector to fit a conventional photoelectron analyzer. We are indebted to Hiroshi Ando of NTT Advanced Technology Inc. for his assistance during these experiments.

*Present address: NTT Basic Research Laboratories, 3-1, Morinosato-Wakamiya, Atsugi-shi, Kanagawa, 243-01, Japan.

†Present address: Department of Applied Chemistry, Graduate School of Engineering, The University of Tokyo, 7-3-1 Hongo, Bunkyo-ku, Tokyo 113, Japan.

[1] A. Abraldi, M. Barnaba, B. Brena, D. Cocco, G. Comelli, S. Lizzit, G. Paolucci, and R. Rosei, J. Electron Spectrosc. Relat. Phenom. **76**, 145 (1995).

[2] F. Maeda, Y. Watanabe, Y. Muramatsu, and M. Oshima, Jpn. J. Appl. Phys. **35**, 4457 (1996).

[3] Y. Muramatsu, F. Maeda, S. Maeyama, Y. Watanabe, and M. Oshima, Nucl. Instrum. Methods Phys. Res., Sect. A **342**, 596 (1994).

[4] A. Shibayama, T. Kitayama, T. Hayasaka, S. Ido, Y. Uno, T. Hosokawa, J. Nakata, K. Nishimura, and M. Nakajima, Rev. Sci. Instrum. **60**, 1779 (1988).

[5] F. Maeda, Y. Watanabe, and M. Oshima, J. Electron Spectrosc. Relat. Phenom. **80**, 225 (1996).